

## An Improved Method of Calculating Flux Coordinates\*

JAMES A. ROME

*Oak Ridge National Laboratory, P.O. Box 2009, Oak Ridge, Tennessee 37831*

Received April 12, 1988; revised July 22, 1988

The twisty nature of stellarator geometry can be “hidden” from many calculations by basing a coordinate system on the twisty flux surfaces. A particularly good choice for this flux coordinate system, developed by A. H. Boozer, has straight field lines and a Jacobian that depends only on the magnitude of the magnetic field, **B**. Boozer’s original method of generating the coordinate system had difficulty in determining the correct harmonics when the rotational transform,  $\iota$  (the number of times a field line twists around the torus in the short direction for each transit in the long direction), is rational ( $\iota = n/m$ ) and when the transform per field period is large. With this improved method, two field lines are used to calculate Boozer’s flux coordinates on a given flux surface. This splits the spectra so that adjacent toroidal mode numbers are assigned to different spectra, and the correct amplitudes of overlapping harmonics can be determined. © 1989 Academic Press, Inc.

### INTRODUCTION

Stellarators are toroidal fusion devices that create magnetic confinement geometries for charged plasma particles. The magnetic field lines twist about a torus on a set of nested surfaces known as flux surfaces. The charged particles travel freely along the magnetic field lines and drift slowly across them because of gradients and curvature of the magnetic field. The rotational transform,  $\iota$ , measures the twist of these field lines about the torus. To make the field lines encircle the torus poloidally (the short way around) without using any current in a plasma, the flux surfaces must be made to assume a twisty, roughly helical shape. Conventional stellarators and torsatrons use sets of magnetic coils, which are wrapped helically about the torus to create the desired magnetic topology. Generally, the coils are periodic in the toroidal angle, resulting in  $N$  field periods, each of which exhibits the same magnetic topology. A complete review of stellarators is given in Reference [1].

To analyze stellarators with unbroken, nested flux surfaces, it is useful to transform into a coordinate system that is based on flux surfaces. In the new coordinate

\* Research sponsored by the Office of Fusion Energy, U.S. Department of Energy, under Contract DE-AC05-84OR21400 with Martin Marietta Energy Systems, Inc. The U.S. Government’s right to retain a nonexclusive royalty-free license in and to the copyright covering this paper, for governmental purposes, is acknowledged.

system, the flux surfaces are nested circular tori, and the geometry appears to be simpler.

Boozer devised a set of flux coordinates [2] for stellarators that have straight field lines; using these coordinates can simplify the physics of orbits as well as increase the speed of calculations. For curl-free magnetic fields, the guiding-center orbit equations in Boozer coordinates (BCs) take a particularly simple form, which depends only on the magnitude of  $\mathbf{B}$ . In addition, the fast motion along a field line is separated from the slower motion across the field lines and flux surfaces.

Previous methods for numerically calculating the BC system [3] had difficulty in two cases: (1) when the surface has a rational rotational transform and (2) when the rotational transform per period ( $\iota/N$ ) is high. In each instance, it becomes difficult to make accurate identification of the Fourier harmonic mode numbers and their amplitudes.

The improved method, embodied in the computer code MAGC2, overcomes these problems by integrating along two field lines; this separates the Fourier spectrum into two spectra, which have separated toroidal mode numbers. As a result, more precise results can be achieved, especially near the last closed flux surface of the plasma.

### BOOZER COORDINATES

Although this discussion specifically concerns the vacuum case, the methods presented here are also valid for finite beta equilibria.

The magnetic field has a covariant representation,

$$\mathbf{B} = \nabla\chi + \beta \nabla\psi, \quad (1)$$

and a contravariant representation,

$$\mathbf{B} = \nabla\psi \times \nabla\theta_0. \quad (2)$$

$2\pi\psi$  is the toroidal flux, and  $\theta_0$  is the label of a field line. Dotting the two representations together gives an equation for the Jacobian,

$$|\mathbf{B}|^2 = \nabla\chi \cdot (\nabla\psi \times \nabla\theta_0). \quad (3)$$

The periodicities of the torus can be made more obvious by introducing a toroidal angle  $\varphi$  and a poloidal angle  $\theta$  related to  $\chi$  and  $\theta_0$  by

$$\chi = g(\psi)\varphi + I(\psi)\theta, \quad (4)$$

$$\theta = \theta_0 + \iota(\psi)\varphi. \quad (5)$$

In these equations,  $g(\psi)$  is  $(\mu_0/4\pi)$  times the total poloidal current outside a flux surface (mks units), and  $I(\psi)$  is  $(\mu_0/4\pi)$  times the total toroidal current inside a flux surface. For the vacuum case,  $I \equiv 0$  and  $g = \text{constant}$ .

Thus, our aim is to find a more accurate method of calculating the BC representation of any quantity of interest. For example, the amplitude of the magnetic field and the real space cylindrical coordinates are given by

$$B(\psi, \theta, \varphi) = \sum_{n,m} B_{mn}(\psi) \cos(nN\varphi - m\theta). \quad (6)$$

$$R(\psi, \theta, \varphi) = \sum_{n,m} R_{nm} \cos(nN\varphi - m\theta), \quad (7)$$

$$Z(\psi, \theta, \varphi) = \sum_{n,m} Z_{nm} \sin(nN\varphi - m\theta), \quad (8)$$

$$\Phi(\psi, \theta, \varphi) - \varphi = \sum_{n,m} \Phi_{nm} \sin(nN\varphi - m\theta), \quad (9)$$

This representation also assumes that the stellarator of interest has the usual reflectional symmetries, that  $\varphi=0$  is defined at a symmetry plane, and that  $\theta=0$  is defined on the equatorial plane; that is, the field line label  $\theta_0$  is defined to be zero at  $\varphi=0, \theta=0$ .  $N$  is the number of field periods in the device of interest.

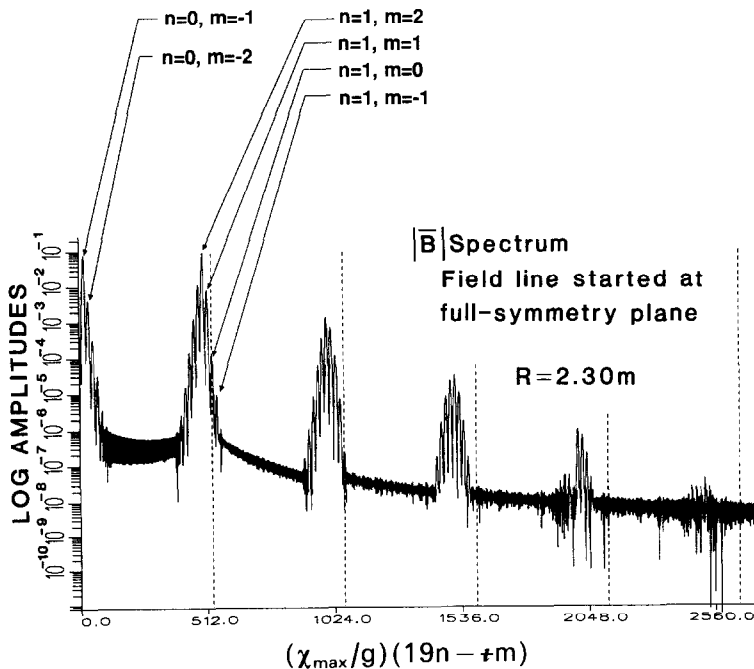


FIG. 1. The amplitudes of the  $|B|$  Spectra started at the two symmetry lines on the same flux surface are essentially identical. The dashed lines are the locations of the  $m=0, n=0, 1, 2, \dots$  harmonics. Above these lines are the  $m=-1, -2, -3, \dots$  harmonics, and below them are the  $m=+1, +2, +3, \dots$  harmonics.

To calculate this set of flux coordinates, Boozer devised a clever method which is local to a flux surface and which does not require that the location of the surface be known a priori. Details are given in Ref. [2], but a brief summary follows. In the vacuum case,  $\chi = \int B dl$  is the scalar potential for the magnetic field. A magnetic field line is integrated around the torus long enough to "cover" the surface, empirically about  $3.5/\epsilon$  times around toroidally.  $\chi$  is the independent coordinate for the integration.

Because the quantity of interest (e.g.,  $|\mathbf{B}|$ ) is only quasi-periodic along the field line, it is necessary to "window" the function by multiplying it by a function that goes to zero at the ends of the sampling interval. A gaussian is particularly suited for this because its Fourier transform is also a gaussian. The windowed function is sampled with enough samples to satisfy the Nyquist criteria, and it is subjected to a 1-dimensional fast Fourier transform (FFT). The resulting spectrum consists of a set of sampled gaussians, as shown in Fig. 1. The peaks of the spectrum occur at positions given by

$$\text{position} = (\chi_{\max}/g)(nN - \epsilon m), \quad (8)$$

where  $\chi_{\max}$  is the length of the original integration along the field line.

The spectrum makes it possible to obtain very accurate values for  $\epsilon$  by finding the best match for all of the peaks in the spectrum.

#### IDENTIFICATION OF SPECTRAL PEAKS

To automatically identify the  $m, n$  values associated with each peak in the spectrum, the following algorithm is employed:

(1) The values of  $g, I$ , and  $\psi$  are calculated using the puncture points (at  $\Phi = \text{constant}$ ) for the flux surface. The puncture points are fitted with a tensioned spline, being sure to enforce the required up/down symmetry. The flux is calculated by doing an area integral over this surface, and the toroidal current ( $\sim I$ ) is calculated using a line integral around this surface.

The calculation of  $g$  is more difficult. During the field line integration, the value of  $\chi = \int B dl$  is stored after exactly one toroidal transit of the machine, together with the associated puncture point. Then the poloidal integral of  $B dl$  is completed from this point to the symmetry point at which the field line was launched. The sum of these integrals is

$$\mu_0 * (\text{poloidal current} + k * \text{toroidal current}),$$

where  $k$  is 1 + the number of complete poloidal encirclements of the field line in one toroidal transit.

(2) Because the windowing function used before taking the FFT is a gaussian of the form

$$\frac{4\eta}{\sqrt{\pi S}} \exp -\frac{1}{2} (\eta\chi)^2,$$

where  $S$  is the number of samples, the resulting spectrum is a series of sampled gaussians of width  $8\eta^2/9.8696044$ . Since the peak of each gaussian does not necessarily correspond to the position of a discrete sample, the peaks near each maximum are fitted to gaussians. This procedure yields more precise determination of the amplitude and position of each peak.

(3) The locations of the  $m=0$  peaks are known (Eq. (7)) without reference to  $\tau$ . An important check of the accuracy of the computer run is obtained by being sure that these positions line up with peaks of the spectrum.

(4)  $\tau$  is determined by using the ten largest peaks (except near the magnetic axis where fewer peaks are used). The distance of each  $m \neq 0$  peak should be an integral multiple of  $(\tau\chi_{\max})/g$  away from the  $m=0$  peaks. The distance between any two peaks determines a trial value for  $\tau$ . The location of each peak is tested against Eq. (7) for the 2-4 nearest  $n$  values, and for (typically)  $-15 \leq m \leq 15$ . The correct value of  $\tau$  is the one that gives the lowest square of the residuals of Eq. (7) for all peaks. Then the value of  $\tau$  is refined by using the values of all of the peaks above some minimum cutoff value.

(5) With  $\tau$  determined, it is straightforward to find the  $m, n$  values for all of the peaks using Eq. (7), except near rational surfaces, as will be discussed below. If there is some uncertainty about the assignment of a given peak, in accord with the fact that the spectra decay with increasing  $m$ , the harmonic is assigned to the closest  $m=0$  peak. Even near rational surfaces, the spectral identification can often be made by using the assignment of the peak on neighboring flux surfaces. This strategy fails near the magnetic axis when the peak emerges from the noise level, and near the edge when the spectra overlap.

#### DIFFICULTIES WITH THE METHOD

If  $\tau = nN/m$  (a rational surface), it becomes difficult to uniquely identify the  $n, m$  values associated with a particular peak. For example, in Heliotron ( $N=19$ ), if  $\tau = 19/12$ , the positions of the peaks for  $n=0, m=12$ , and  $n=1, m=0$  coincide.

Ordinary, as shown in Fig. 1, the harmonics decay for increasing  $|m|$ , although, as shown, the largest harmonic associated with a given  $n$  moves to lower frequencies as  $n$  is increased. If  $\tau/N$  is small, the peaks associated with each  $n$  value are isolated. However, for a high-transform machine such as Heliotron or the heliacs, if  $\tau/nN \approx m$ , the spectra will overlap and the individual gaussian peaks will combine. Estimates of the amplitudes of the two overlapping peaks can be completely wrong if a small peak lies on top of a large one.

There is yet another difficulty with using Boozer's method on rational surfaces. It is necessary to do integrals along the surface to find  $g$  and  $I$  and to do area integrals of the surface to determine the toroidal flux,  $\psi$ . Rational surfaces separate the puncture points and make these integrals more inaccurate. For heliac configurations, the connectivity of these points can be difficult to determine automatically.

### SPLITTING THE SPECTRUM

As stated earlier, to generate flux coordinates, it is important to select a field line that starts at a symmetry point on each flux surface. In addition to reducing the Fourier series to either a sine or a cosine series (according to whether the function is odd or even), this choice is also required to relate the coefficients on one surface to those on neighboring surfaces. Because the real-space coordinates can be expressed in BCs using Eqs. (7)–(9), we know a priori that  $\Phi = \varphi$  and that  $Z = 0$  when  $\varphi = 0$  and  $\theta = 0$ . Thus, there is really a line of symmetry (with a point on each flux surface) along which the field line integration can be begun.

An additional question involves the value of  $\chi$  at the beginning of the field line on this symmetry line. If  $\chi$  were other than a constant independent of  $\psi$ , there would be a  $\psi$  component of  $\mathbf{B}$ . We know that there can be no  $\psi$  component of  $\mathbf{B}$  on the symmetry line, so the constant is independent of  $\psi$  and we can set it to zero. Finally, there are two symmetry planes per field period for stellarators of interest, thus, two symmetry lines can be used. One symmetry line occurs (for a conventional torsatron) underneath the helical coil at the  $\Phi$  where the coil crosses the equatorial plane. The other is halfway between the helical coils, also on the equatorial plane. Thus, for the 19 field period Heliotron-E, the planes occur at  $\Phi = 0$  and  $\pi/19$ .

One might ask "What is the relationship of the amplitudes of the Boozer harmonics obtained from the two choices of symmetry line?" Since  $\theta$  is the same for each starting point and  $\varphi$  is slipped by half of a field period, the relationship is

$$A_{nm}^1 = (-1)^n A_{nm}^2, \quad (11)$$

where  $A_{nm}$  represents the  $n, m$  harmonic for any quantity of interest. If we add the two resulting spectra, we will have only harmonics corresponding to  $n = 0, 2, 4, \dots$ ; if we subtract them, we will obtain the harmonics corresponding to  $n = -1, 1, 3, 5, \dots > 0, m > 0$  location<sup>1</sup>

The net effect of adding and subtracting the spectra is to spread out the harmonics, avoiding spectral overlap. Figure 1 illustrates the spectra for  $|\mathbf{B}|$

<sup>1</sup> We included  $-1$  in the latter spectra because we use the spectrum only for positive frequencies. Terms with  $n = -1$  and with  $m$  large and negative can occur at positive frequencies. After the harmonic is identified, it is assigned to its correct  $n$ .

obtained by integrating along the  $\Phi=0$  field line. The amplitude spectrum at  $\Phi=\pi/19$  is essentially identical. To illustrate the process more clearly, we have chosen an interior flux surface for a model Heliotron-E (based upon toroidal corrections to a straight stellarator [4], where the harmonics are already well separated. Figure 2 displays the sum spectrum and the difference spectra. The method reduces the cancelling terms in this case by three to four orders of magnitude. The peaks that add have the average of the amplitudes and positions of the peaks from each of the two spectra.

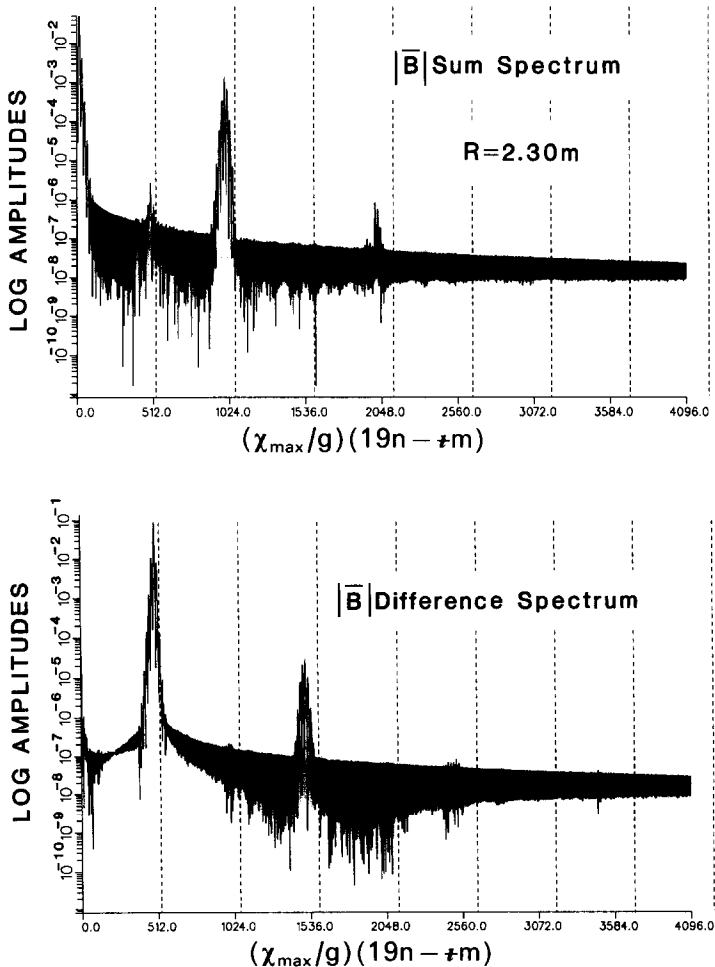


FIG. 2. The sum spectrum has harmonics for only even values of the toroidal mode number  $n$ . The difference spectrum has harmonics for only odd  $n$ .

ERROR CONSIDERATIONS

When double precision is used on a VAX computer, this method of deriving the BCs has a dynamic range of about six orders of magnitude. To maintain this range, the average ( $m=0, n=0$ ) term is always subtracted before the FFT is performed. The reduction in amplitude of the unwanted peaks in the sum or difference spectra is usually two or three orders of magnitude. The two-field-line method depends crucially on the condition that both field lines are really on the same flux surface. Accordingly, after the first field line is integrated, a puncture plot of the half-symmetry plane is produced, and the starting point in this plane is determined. This is discussed in more detail in the section entitled "Rational Surface Considerations."

The reduction in the amplitude of the unwanted peaks is quite sensitive to the proximity of the second field line to the first flux surface; however, the peaks that add are quite insensitive. Thus, a method for discriminating against unwanted peaks is required.

The primary method for automatically accepting peaks and assigning them to their correct  $A_{nm}$  is to examine the frequency of the peak. The frequency must line up closely with the frequencies given in Eq. (7). In the two-field-line method, the peaks in the sum spectra are assigned only to even  $n$ , and those in the difference spectra are assigned only to odd  $n$ . Remarkably, the small peaks that result from the cancellation of two large peaks often line up with the correct peak locations for the  $n$  to either side of the unwanted  $n$  values. These peaks are clearly spurious

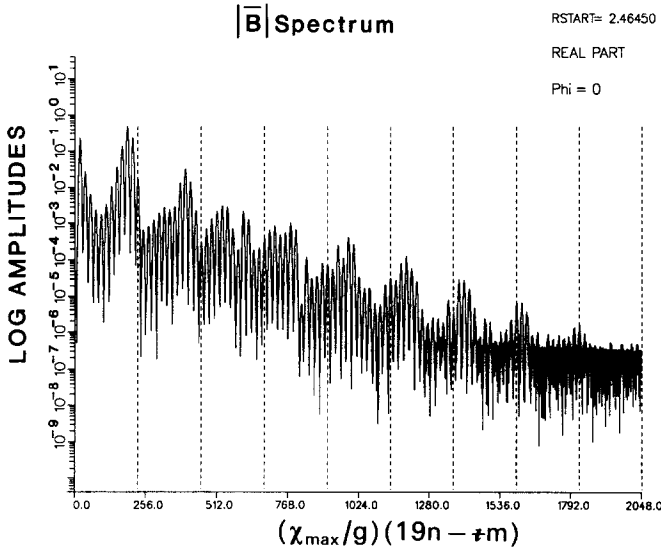


FIG. 3. The  $|B|$  spectrum on a near rational surface ( $\pm \sim \frac{19}{12}$ ) near the edge of the plasma is quite complicated. The harmonics for different  $n$  overlap, and the spacing between all peaks is a multiple  $\pm/g$ .



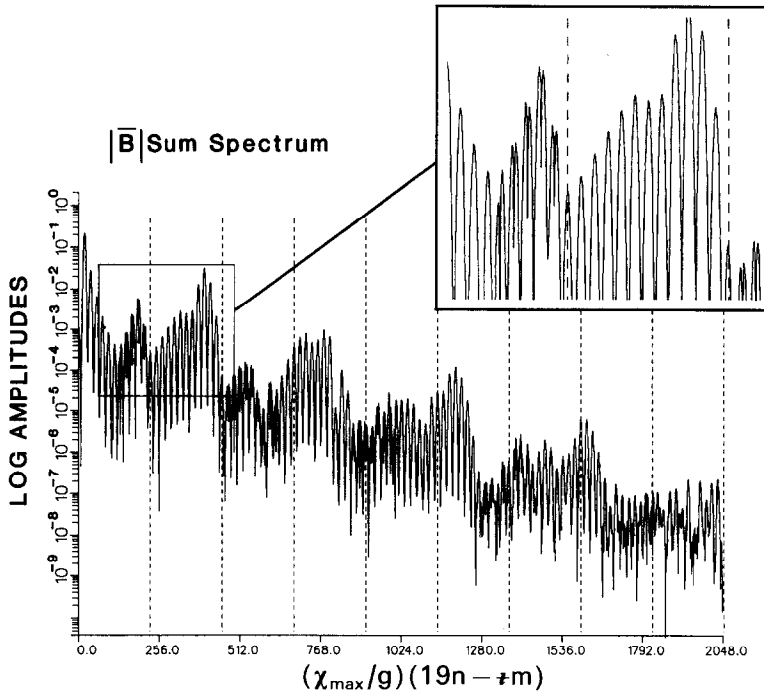


FIG. 4. For  $\dagger \sim \frac{19}{12}$ , the sum spectrum reduces the amplitudes of peaks corresponding to odd  $n$  by almost 2 orders of magnitude. As shown in the inset, the width of these unwanted peaks is much narrower, allowing them to be discriminated against. Note that the reduced value of the  $n=2$ ,  $m=12$  peak has been correctly uncovered from underneath the  $n=1$ ,  $m=0$  peak.

because their amplitudes vary wildly according to the closeness of the match of the two flux surfaces and are small in any event. Fortunately, their width is much narrower than that of the correct peaks. Since the width of the gaussian peaks is known analytically, it is a simple chore to reject any peaks that are narrower than, for example, 75% of the correct width.

Figure 3 shows the  $|\mathbf{B}|$  spectrum on a near-rational ( $\dagger \approx \frac{19}{12}$ ) outer flux surface for this model Heliotron-E field (which has a lower  $\dagger$  than the real machine). The spectrum is quite complicated, and the harmonics for different  $n$  overlap. In the sum spectrum of Fig. 4, the desired peaks are the wide ones, and the rejected peaks are the narrow ones. Consider, for example the  $n=1$ ,  $m=0$  and  $n=2$ ,  $m=12$  harmonics. The both lie on the first vertical dashed line, but the latter peak's amplitude of about  $2 \times 10^{-4}$  has been "pulled out" from underneath the first peak's larger amplitude of about  $2 \times 10^{-2}$ . Similarly, the difference spectrum of Fig. 5 allows more accurate determination of the  $n=0, 3, 5, \dots$  harmonics.

Figure 6 shows the automatically assigned harmonic spectrum for this case, and

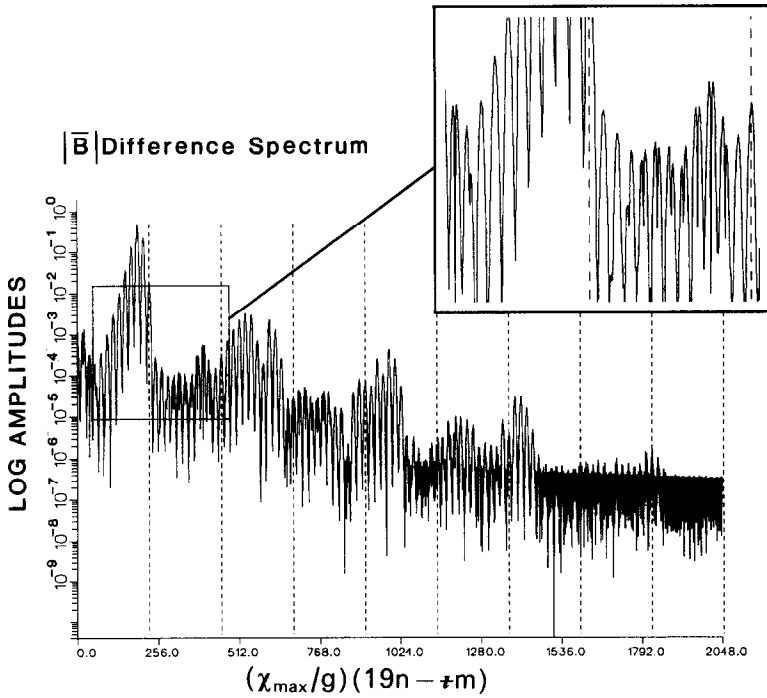


FIG. 5. For  $\tau \sim \frac{19}{12}$ , the difference spectrum determines the correct amplitudes of harmonics such as  $n = 1, m = 6, 7, 8$  and  $m = -1, -2$ .

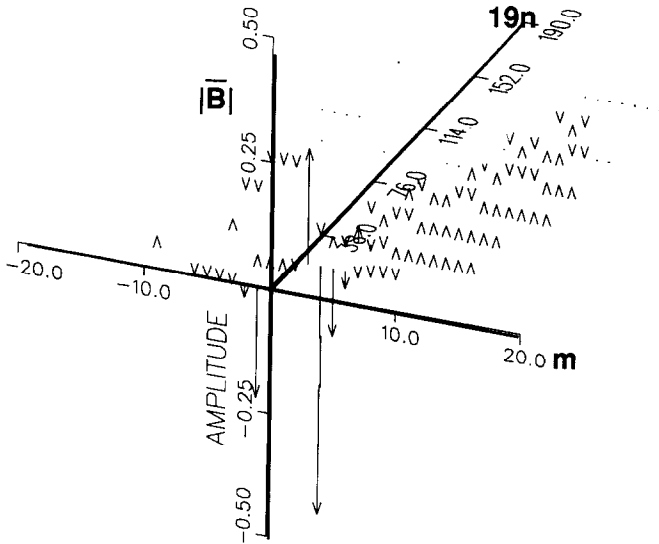


FIG. 6. Classification of harmonics. MAGC2 uses the information from both field lines to provide more accurate assignment of the  $n$  and  $m$  values to each peak of the Fourier spectrum.

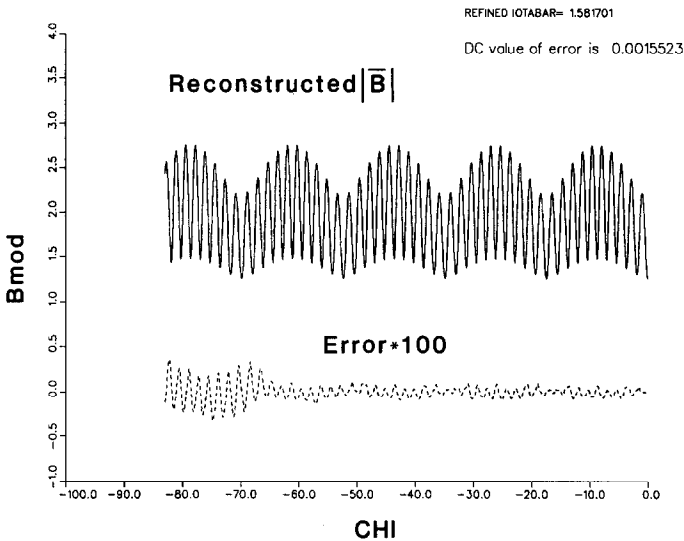


FIG. 7. The magnetic field along the field line can be reconstructed from the harmonics and compared with the original to determine the error.

Fig. 7 shows the reconstructed  $|\mathbf{B}|$  along the field line and the resulting error. Thus, when two field lines are used, assigning the correct  $n$ ,  $m$  values is a much easier and more accurate chore than if only one field line were used.

#### RATIONAL SURFACE CONSIDERATIONS

The preceding strategies serve well for assigning the correct  $n$ ,  $m$  values to the harmonics on near rational surfaces, but correctly calculating  $\psi$ ,  $g$ , and  $I$  and the starting point for the second field line proves to be tricky. Figure 8 shows the puncture points (circles) of the first field line at the two  $\Phi$  symmetry planes for the surface where  $\tau \approx \frac{19}{12}$ . The first field line was started at  $R = 2.4645$  m. No puncture points can be seen near the midplane at the outside of the flux surface. The solution to this dilemma is to fit a tensioned spline to the data points (solid curve). The  $\times$  is the selected location for the start of the second field line.

Because the spline would pass through all of the data points, it would cause oscillations in the fitted curve if all of the data points were used, especially if they were to occur in clumps. We apply an algorithm that uses only data points more than a given distance apart. In addition, only the points for  $Z > 0$  are used; the surviving points are reflected in  $Z$  to enforce symmetry. We then use the routines KURVP1 and KURVP2 from FITPACK, a computer code devised by A. K. Cline and R. J. Renka of the University of Texas at Austin. The tension parameter is set to 1. The success of the method is judged by how well the cancelling harmonics are reduced.

OTHER IMPROVEMENTS IN THE METHOD

Even small errors in  $g$  or  $\tau$  will accumulate and lead to secular error growth over long orbit integration periods. We have two methods for combating this. The value of  $g(\psi)$  is adjusted until the average value of  $\Phi - \chi/g$  ( $\varphi = \chi/g$  in the vacuum case) is as close to zero as possible before the Fourier decomposition of  $\Phi - \varphi$  is performed. Then,  $|\mathbf{B}|$  is reconstructed from its Fourier harmonics and  $\tau$  is varied slightly until the secular growth of the average error is reduced. Values of  $\tau$  good to five significant figures can be achieved in this manner.

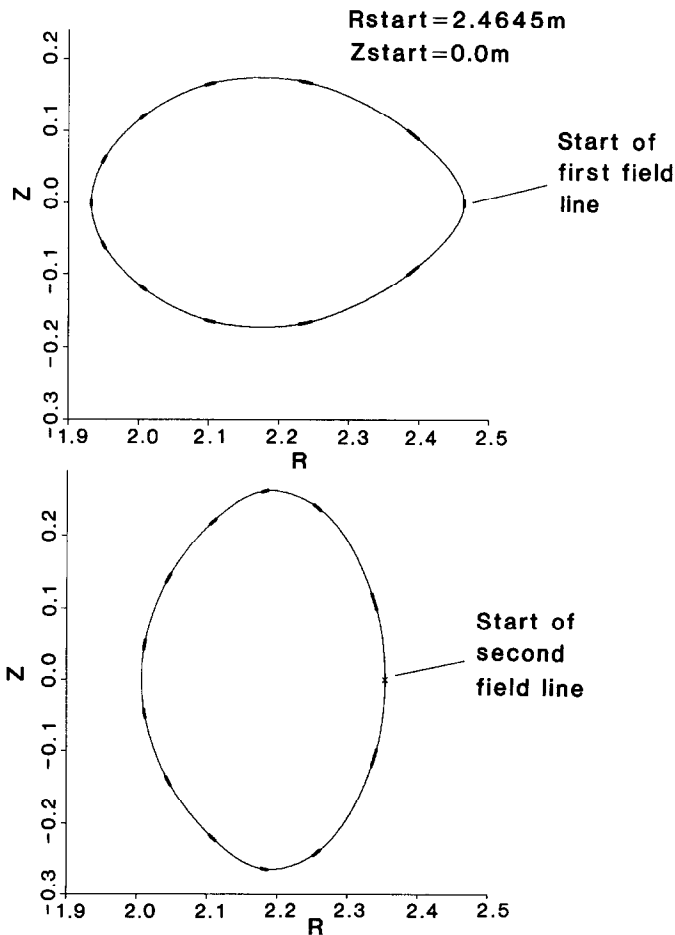


FIG. 8. Puncture plots in each symmetry plane for the rational surface near  $\tau = \frac{19}{12}$  in the model Heliotron-E. The solid lines are the fits achieved with the tensioned spline routine KURVP1 using a tension parameter of 1.0.

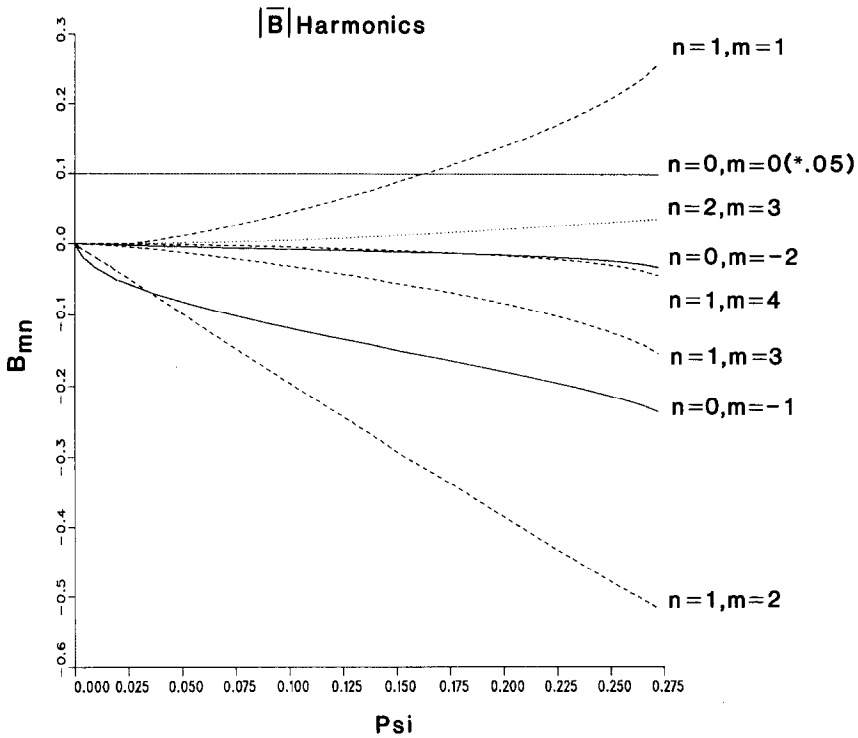


FIG. 9. The  $|\mathbf{B}|$  harmonics for the model Heliotron-E. Only the largest harmonics are shown, and the  $dc$  term is multiplied by 0.05.

#### SUMMARY AND CONCLUSIONS

This improved method for calculating Boozer's flux coordinates overcomes several limitations of previous methods. Figure 9 displays the set of harmonics for  $|\mathbf{B}|$  (the  $dc$  term is multiplied by 0.05). The harmonics display the smoothness in  $\psi$  that is required for the  $\psi$  derivatives of the harmonics in the orbit equations. Also, there is no misassignment of harmonics, even on the outer flux surfaces.

On a VAX 8600, it takes 2–3 cpu h to calculate the Boozer coordinates on 20 flux surfaces if the Biot–Savart law is used to calculate the magnetic field from wire filaments. For the present analytic field, the calculation took about 1 h. It should be pointed out that with this method, the length of field line that is followed does not increase if the flux surface is near rational; each field line is followed for about 3.5+ toroidal transits.

## ACKNOWLEDGMENTS

It is a pleasure to acknowledge useful discussions with Allen Boozer, Ron Fowler, Steve Hirshman, and Robert Morris. Many of the numerical algorithms in the code were provided by Ron Fowler. The model Heliotron field routines were written by Kiyoshi Hanatani.

## REFERENCES

1. B. A. CARRERAS, G. GRIEGER, J. H. HARRIS, J. L. JOHNSON, J. F. LYON, O. MOTOJIMA, F. RAU, H. RENNER, J. A. ROME, K. UO, M. WAKATANI, AND H. WOBIG, *Nucl. Fusion* **28**, 1613 (1988).
2. A. H. BOOZER, *Phys. Fluids* **23**, 904 (1980).
3. G. KUO-PETRAVIC, A. H. BOOZER, J. A. ROME, AND R. H. FOWLER, *J. Comput. Phys.* **51**, 261 (1983).
4. K. MIYAMOTO, *Plasma Physics for Nuclear Fusion* (MIT Press, Cambridge, MA, 1980), p. 29.